Journal of Zhejiang University-SCIENCE A (Applied Physics & Engineering)
ISSN 1673-565X (Print); ISSN 1862-1775 (Online)
www.zju.edu.cn/jzus; www.springerlink.com
E-mail: jzus@zju.edu.cn

A precise solution for prediction of fiber-reinforced concrete behavior under flexure

R. AHMADI[1], P. GHODDOUSI[2], M. SHARIFI[†‡2], V. Mojarrad BAHREH[3]

(*[1]Building and House Research Center, Tehran 13145-1996, Iran*)

(*[2]Department of Civil Engineering, Iran University of Science and Technology, Tehran 16846-13114, Iran*)

(*[3]Department of Civil Engineering, Sharif University of Technology, Tehran 11365-11155, Iran*)

[†]E-mail: mahdysharify@gmail.com

Received Apr. 21, 2010; Revision accepted Oct. 9, 2010; Crosschecked June 21, 2011

Abstract: This paper presents a precise solution to predict the behavior of steel fiber reinforced concrete (SFRC) under the four point bending test (FPBT). All the force components at the beam section (before and after cracking) are formulated by applying these assumptions: a realistic stress-strain model is used for concrete behavior in compression, a linear response is considered for the uncracked tension region in a concrete constitutive model, and an exponential relationship is proposed as a stress-crack opening in the crack region which requires two parameters. Then the moment capacity of the critical cracked section is calculated by using these forces and satisfying equilibrium law at the section. Parametric studies are done on the behavior of SFRC to assess the sensitivity of the solution. Finally, this solution is validated with some existing experimental data. The result shows the proposed solution is able to estimate the behavior of SFRC under FPBT.

Key words: Steel fiber reinforced concrete (SFRC), Flexure, Stress-crack opening, Four point bending test (FPBT)
doi:10.1631/jzus.A1000193 **Document code:** A **CLC number:** TU528

1 Introduction

Concrete is a relatively brittle material, and the mechanical behavior of concrete structures is critically influenced by crack propagation. Cement-based materials easily crack due to applied stress, restraint, or environmental conditions because of their low fracture toughness. Reinforcement of cement-based materials with short, randomly-distributed fibers has been successfully used in recent years, primarily for tunnel linings, industrial floor slabs, and similar applications (Mobasher and Shah, 1989; Mobasher and Li, 1996; Li, 2002).

Nowadays, the question of how to evaluate the flexural toughness and to express it as a useful parameter for design purposes is still under debate (Stang and Li, 2004). A number of test methods have been proposed to evaluate steel fiber reinforced concrete (SFRC) toughness, but all have significant problems associated with either the variability of the results or their application in structural design calculations (Banthia and Trottier, 1995). Also, some attempts have been made for modeling the flexural behavior of SFRC, but none of the models has been able to fully explain what actually happens at the critical cracked section in terms of the fiber-matrix interactions. Consequently, there is a current limitation on the structural use of fiber reinforced material.

Available methods for modeling the flexural post-crack behavior of SFRC are based on the equilibrium of forces at the cracked section. The main concern in these methods, is evaluating the tensile strength at the crack area, which is supported by fibers bridging. Some methods have used a stress-crack opening model from direct uni-axial tensile

[‡] Corresponding author

tests or existing relationship (RILEM TC 162-TDF, 2001; Zhang and Stang, 1998; Abdalla and Karihaloo, 2004). There is no available uni-axial tensile test method currently (van Mier and van Vliet, 2002). Also, using the relationship needs iterative solution to determine the required parameters. Other methods implement the average response of the load transmitted by the fibers through the cracked region from the pull-out tests of single fibers (Armelin and Banthia, 1997; Prudencio *et al.*, 2006; Oh *et al.*, 2007). Some problems arise with these approaches. For example, the number and position of the fibers bridging the crack are not precise, and also the load supported by each fiber depends on the crack opening displacement, the orientation of the fiber, and the embedment length.

This paper deals with a precise solution for predicting the behavior of SFRC under the four point bending test (FPBT). A realistic stress-strain model is used for concrete behavior in compression, and a linear response is considered for uncracked tension region as a concrete constitutive model. An exponential relationship is proposed as a stress-crack opening in the crack region governed by two parameters. All the force components at the beam section (before and after cracking) are formulated by applying these assumptions. Then the moment capacity of the critical cracked section is calculated by using these forces and the satisfying equilibrium law at the section. Parametric studies are done on the behavior of SFRC to assess the sensitivity of the solution. Finally, this solution is validated with existing experimental data.

2 Model concepts

An idealized representation of the strain and stress block diagram at the critical cracked section of a steel fiber reinforced concrete beam under flexural loading is shown in Fig. 1. The developed stresses and resultant forces at the critical section can be represented by three separate zones, including a compression zone, an uncracked tension zone, and a cracked tension zone. The cracked tension zone shows the aggregates interlock and fibers bridging. Consequently, the flexural capacity of the critical section is a function of the following principal parameters: (1) the concrete compressive stress-strain relationship; (2) the concrete tensile stress-strain relationship; (3) the concrete crack opening relationship; (4) the strain profile and related neutral axis location of uncracked and cracked sections; (5) crack width profile associated with mid-span deflection.

Therefore, it is necessary to specify the required relationships for the aforementioned parameters in order to predict the shape and magnitude of the stress-block diagram for a given beam deflection.

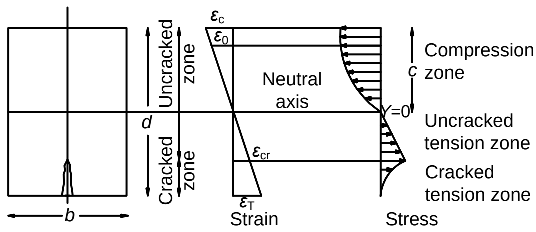

Fig. 1 Strain and stress distribution on the cracked section
b: section width; d: section depth; ε_c: compressive strain at top fiber; ε_T: tensile strain at bottom fiber; ε_{cr}: cracking strain; ε_0: compressive strain at f_c'

2.1 Concrete constitutive model

In this study, the Hognestad's stress-strain relationship is used for concrete behavior in compression (Park and Paulay, 1975). This is one of the most generally used equations to model the constitutive behavior of concrete. The typical stress-strain relationship of this model is shown in Fig. 2. Based on this model, the stress-strain relationship of concrete in compression is expressed by

$$f_c = f_c'[(2\varepsilon_c / \varepsilon_0) - (\varepsilon_c / \varepsilon_0)^2], \quad 0 \le \varepsilon_c \le \varepsilon_0, \tag{1}$$

$$f_c = f_c'[1 - 0.15(\varepsilon_c - \varepsilon_0) / (0.004 - \varepsilon_0)], \quad \varepsilon_c \ge \varepsilon_0, \tag{2}$$

where f_c is the compressive stress in section, f_c' is the compressive strength of concrete, ε_c is the compressive strain, ε_0 is the compressive strain corresponding to f_c', and $\varepsilon_0 = 2f_c'/E_c$, where E_c is the elastic module of concrete.

A linear response is considered for tensile behavior of concrete at the uncracked zone.

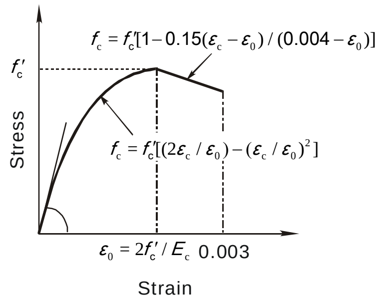

Fig. 2 Concrete constitutive model in compression (Park and Paulay, 1975)

2.2 Crack opening relationship

In this study, an exponential relationship F_f with two parameters is proposed to present the crack-opening stress:

$$F_f = f_t e^{\beta w}, \quad \beta < 0, \tag{3}$$

where w is the crack opening width, f_t is the tensile strength, β is a coefficient that represents the intensity of descending part of relationship, and f_t and β are two basic parameters of the model. This model is simple and can be easily formulated. The curve of F_f/f_t in function of β is shown in Fig. 3a. The value of parameter β depends on fiber, matrix, and fiber-matrix

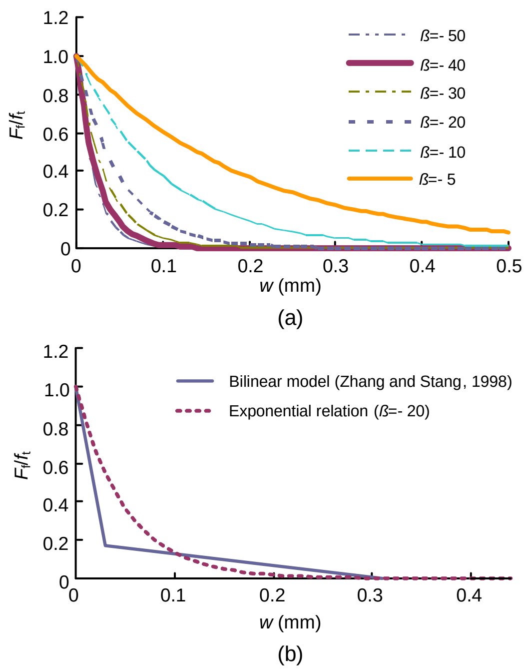

Fig. 3 Proposed model for crack opening stress as a function of β (a) and its comparison with another model (b)

interface properties, and can be derived from the validation of the bending test results as presented in Section 3. A comparison of the proposed model with the bilinear model used in Zhang and Stang (1998) is presented in Fig. 3b. As shown in Fig. 3b, the model can describe the tension softening regime of concretes with proper accuracy.

2.3 Crack tip opening width-mid span deflection relationship

It is necessary to make some assumptions in order to obtain the profile of the curve relating the crack tip opening (w_0) to the mid-span deflection (δ) in a flexural test. The elastic deflections of the specimen in standard FPBT are of the order of hundredths of a millimeter while the desirable region of the load versus deflection diagram for calculating the toughness indices lies in a range of deflections from 10 to 100 times greater than those at the first crack, i.e., up to 2 mm (JCI SF4, 1983; ASTM C1018-97, 1997). This implies that the rigid body motion of the two broken halves of the specimen shows the dominant mechanism. Thus, the failure mode commonly observed, characterized by a main failure crack at mid-span and the cracked portion at central location, acts as a plastic hinge.

Armelin and Banthia (1997) proposed a simple solution assuming the axial compressive strain at the top-most fiber of the specimen at mid-span (ε_t) as a function of the rotation angle. The total axial shortening (Δ_0) can be computed from Fig. 4 as

$$\Delta_0 = \int_0^L \varepsilon_x \mathrm{d}x = 2/3\varepsilon_t L, \tag{4}$$

where ε_x is the axial compressive strain at the top-most fiber along the specimen, and L is the specimen length. The deflection at central position is obtained from the slope of the beam as follows:

$$\delta = \theta \frac{L}{2}, \tag{5}$$

where θ is the angle of the two broken halves of the specimen with the horizontal axis (Fig. 4).

The linear crack profile is reasonably assumed here in the bending region. The crack width opening displacement (w_0) at the bottom fiber is written as

$$w_0 = 2\theta(d-c), \tag{6}$$

where d and c are the section and the compressive zone depths, respectively.

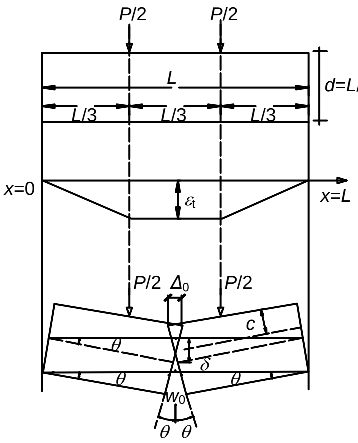

Fig. 4 Failure mode of fiber reinforced concrete beam in the four point bending test
P: axial load; ε_t: axial strain of top fiber

2.4 Model formulation

Considering the former relationships, the stresses and forces at the cracked section can be created in three stages as shown in Fig. 5. All the force components at the beam section are formulated in this section for three stages.

2.4.1 Equations for stage 1 (uncracked section)

The compressive force of uncracked section is obtained by the following equation evaluated in specified compression strain field:

$$F_c = \int_0^{Y_c} \sigma_c b \mathrm{d}y = \int_0^{Y_c} f_c' \left[\left(\frac{2\varepsilon_c}{\varepsilon_0} \right) - \left(\frac{\varepsilon_c}{\varepsilon_0} \right)^2 \right] b \mathrm{d}y, \tag{7}$$

where f_c', σ_c, b, and Y_c are the compressive strength, compressive stress, width of section, and compressive zone depth, respectively.

Substituting Eq. (8) into Eq. (7), one obtains

$$Y / Y_0 = \varepsilon / \varepsilon_o, \tag{8}$$

$$\begin{aligned} F_c &= \int_0^{Y_c} f_c' [2Y/Y_0 - (Y/Y_0)^2] b \mathrm{d}y \\ &= f_c' b [Y_c^2 / Y_0 - Y_c^3 / (3Y_0^2)], \end{aligned} \tag{9}$$

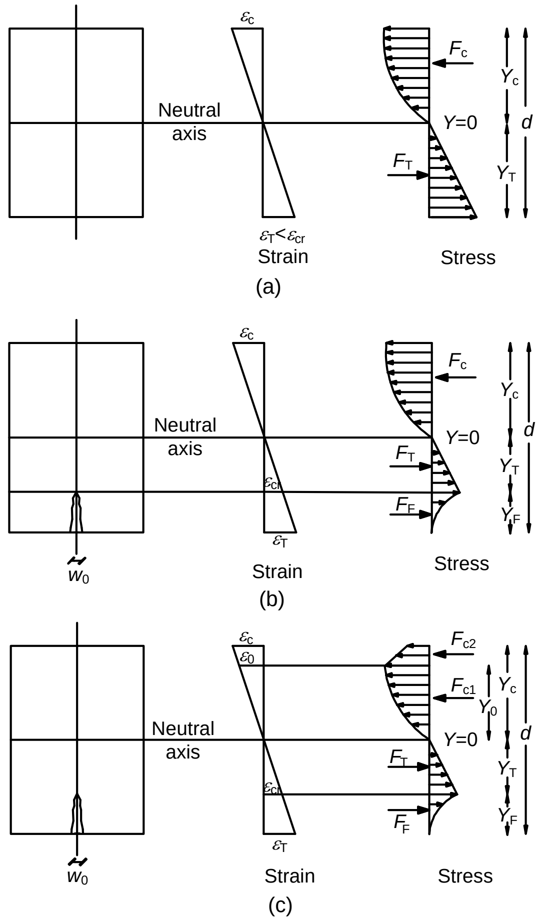

Fig. 5 Stress and force in section
(a) Stage 1 before cracking; (b) Stage 2 in the cracked section; (c) Stage 3 in the cracked section

where Y_0 is the compressive depth corresponding to f_c', and ε is the strain at section of beam.

The tensile force of uncracked section is also calculated as follows:

$$F_T = \int_0^{Y_T} \sigma_T b \mathrm{d}y = \frac{1}{2} E \varepsilon_T Y_T b, \tag{10}$$

where E, σ_T, ε_T, and Y_T are the module of elasticity, tensile stress, tensile strain, and uncracked tension zone depth, respectively.

Now considering the equilibrium law (F_c=F_T), the neutral axis position should be determined by changing the depth of compression region in a specified compression strain. The moment capacity of section is also calculated as

$$M_{\text{Total}} = M_T + M_c, \tag{11}$$

where M_T and M_c are the moments due to tensile and compressive stress about the neutral axis, and are calculated as

$$M_{\mathrm{c}}=\int_0^{Y_{\mathrm{c}}}\sigma_{\mathrm{c}}by\mathrm{d}y=\int_0^{Y_{\mathrm{c}}}f_{\mathrm{c}}'\left[\left(\frac{2Y}{Y_0}\right)-\left(\frac{Y}{Y_0}\right)^2\right]by\mathrm{d}y =f_{\mathrm{c}}'b\left[\frac{2Y_{\mathrm{c}}^3}{3Y_0}-\frac{Y_{\mathrm{c}}^4}{4Y_0^2}\right], \quad (12)$$

$$M_{\mathrm{T}}=\int_0^{Y_{\mathrm{T}}}\sigma_{\mathrm{T}}by\mathrm{d}y=\frac{1}{2}E\,\varepsilon_{\mathrm{T}}\,Y_{\mathrm{T}}\,Y_{\mathrm{T}}\,b=\frac{1}{3}b\,f_{\mathrm{T}}\,Y_{\mathrm{T}}^2. \quad (13)$$

2.4.2 Equation for stage 2 (cracked section)

Stage 2 begins while the tensile stress at the bottom fiber of the beam reaches its strength. In this case, the concrete forces in compression and tension area can be computed from Eqs. (9) and (10).

The force in the cracked region can be calculated by carrying out the integral of the proposed exponential relation F_f over the cracked depth as

$$F_{\mathrm{F}}=\int_0^{Y_{\mathrm{F}}}f_{\mathrm{t}}\mathrm{e}^{\beta w}b\mathrm{d}y=\int_0^{Y_{\mathrm{F}}}f_{\mathrm{t}}\mathrm{e}^{\beta Y\theta}b\mathrm{d}y=\frac{b\,f_{\mathrm{t}}}{\beta\theta}(\mathrm{e}^{\beta Y_{\mathrm{f}}\theta}-1), \quad (14)$$

where F_F, f_t, and Y_F are the tensile force at the cracked zone, tensile strength, and cracked zone depth, respectively.

Now considering the equilibrium law at the cracked section, one obtains

$$F_{\mathrm{c}}=F_{\mathrm{F}}+F_{\mathrm{T}}, \quad (15)$$

which will be used to determine the neutral axis position by changing the depth of the compression region in specified compression strain.

The moment capacity of the section can be obtained with the equilibrium law in Eq. (15):

$$M_{\mathrm{Total}}=M_{\mathrm{T}}+M_{\mathrm{c}}+M_{\mathrm{F}}, \quad (16)$$

where M_F is the moment of the cracked zone, and is calculated as

$$M_{\mathrm{F}}=\int_0^{Y_{\mathrm{F}}}f_{\mathrm{t}}\mathrm{e}^{\beta w}by\mathrm{d}y+F_{\mathrm{F}}\,Y_{\mathrm{T}} =b\,f_{\mathrm{t}}\left(\frac{Y_{\mathrm{F}}\,\mathrm{e}^{\beta Y_{\mathrm{F}}\theta}}{\beta\theta}-\frac{\mathrm{e}^{\beta Y_{\mathrm{F}}\theta}}{\beta^2\theta^2}+\frac{1}{\beta^2\theta^2}\right)+F_{\mathrm{F}}\,Y_{\mathrm{T}}. \quad (17)$$

2.4.3 Equation for stage 3

While the compressive strain of concrete reaches ε_0, it is necessary to rewrite Eq. (7), and consequently, Eq. (9) in stage 3 will be changed as follows:

$$F_{\mathrm{c}}=F_{\mathrm{cp}}+F_{\mathrm{cl}}, \quad (18)$$

where F_{cp} and F_{cl} represent two compression forces:

$$F_{\mathrm{cp}}=f_{\mathrm{c}}'b[Y_0^2/Y_0-Y_0^3/(3Y_0^2)]=\frac{2}{3}f_{\mathrm{c}}'b\,Y_0, \quad (19)$$

$$F_{\mathrm{cl}}=\int_{Y_0}^{Y_{\mathrm{c}}}f_{\mathrm{c}}'\left[1-\frac{0.15(\varepsilon_{\mathrm{c}}-\varepsilon_0)}{0.004-\varepsilon_0}\right]b\mathrm{d}y =\int_{Y_0}^{Y_{\mathrm{c}}}f_{\mathrm{c}}'\left[1-\frac{0.15\left(Y\,\varepsilon_0/Y_0-\varepsilon_0\right)}{0.004-\varepsilon_0}\right]b\mathrm{d}y =f_{\mathrm{c}}'b\left[Y_{\mathrm{c}}-\frac{0.15\varepsilon_0}{0.004-\varepsilon_0}\left(\frac{Y_{\mathrm{c}}^2}{2Y_0}-Y_{\mathrm{c}}\right)\right]. \quad (20)$$

It should be noted that the ordinary fibrous concrete never experiences this stage.

Now the load-deflection curve can be generated by the following step by step procedure as shown in Fig. 6.

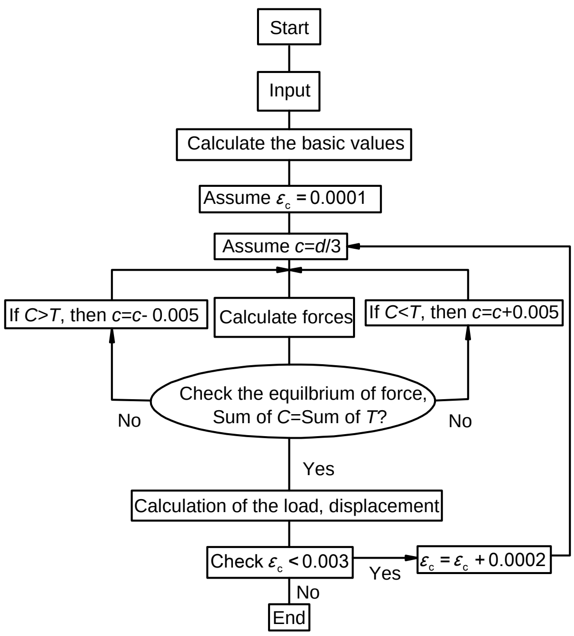

Fig. 6 Step by step procedure for generating the load-deflection curve

C: compressive force; *T*: tension force; *c*: compressive depth; *d*: depth of section

3 Parametric study

Two sets of parametric studies were conducted to assess the sensitivity of the model. Fig. 7 presents the parametric study of FRC materials with different crack opening relationships for a specified concrete with $f_c' = 45$ MPa, f_t=4.5 MPa, and E=33 GPa.

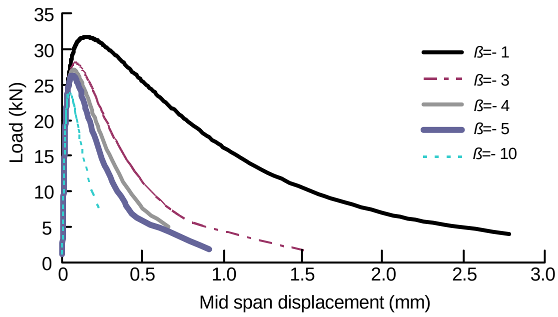

Fig. 7 Load-deflection for fiber reinforced concrete material in function of β

Another parametric study is done for two sets of FRC material with the same crack opening relationship and different model parameters in tensile strength and elastic modulus. The result is shown in Fig. 8.

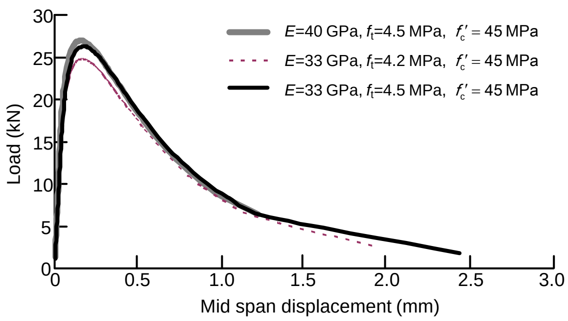

Fig. 8 Load-deflection for fiber reinforced concrete material in function of f_t and E

4 Model validation

The proposed model is validated using some existing experimental results. Balaguru and Najm (2004) performed an experimental investigation on the flexural behavior of high-performance FRC with fiber volume fractions up to 3.75% for seven mixtures. The predicted behavior of mixture 7 of the proposed model has been compared with their experimental results (Fig. 9).

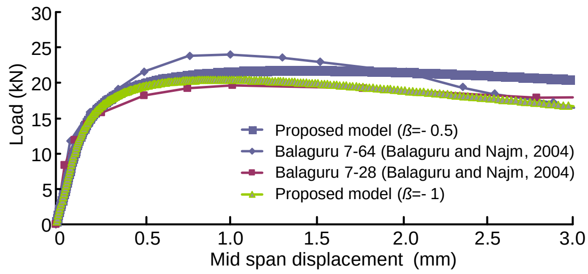

Fig. 9 Comparison of the experimental data (Balaguru and Najm, 2004) with the proposed model

Another validation is done with the results of Zhang and Stang (1998). They investigated the application of the stress crack opening relationship in predicting the flexural behavior of FRC. The comparison of the proposed model with their results for one set of data has been shown in Fig. 10.

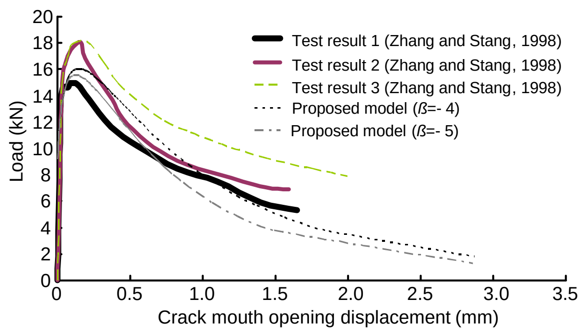

Fig. 10 Comparison of the experimental data (Zhang and Stang, 1998) with the proposed model

5 Model development

This section discusses about how this model can be developed in the presence of an initial axial load as the initial condition (Fig. 11).

In the presence of an initial axial load, it is necessary to revise the model formulation (Section 2.4) as follows:

1. There is an initial strain (ε_i) in the section due to applied axial load of P_1.

2. The stage 1 in Section 2.4.1 and its related stress and forces (Fig. 5a) will change into two states: compression state and compression-tension state (Fig. 12).

In compression state, the section is under full compressive stress, and its related force is calculated by

$$F_c = \int_{Y_c-d}^{Y_c} \sigma_c b\mathrm{d}y = \int_{Y_c-d}^{Y_c} f_c'[2\varepsilon_c/\varepsilon_0-(\varepsilon_c/\varepsilon_0)^2]b\mathrm{d}y. \quad (21)$$

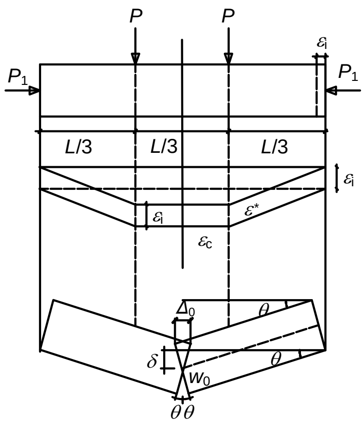

Fig. 11 Beam under axial load and bending moment

ε_i: strain due to initial load; ε^*: strain due to bending

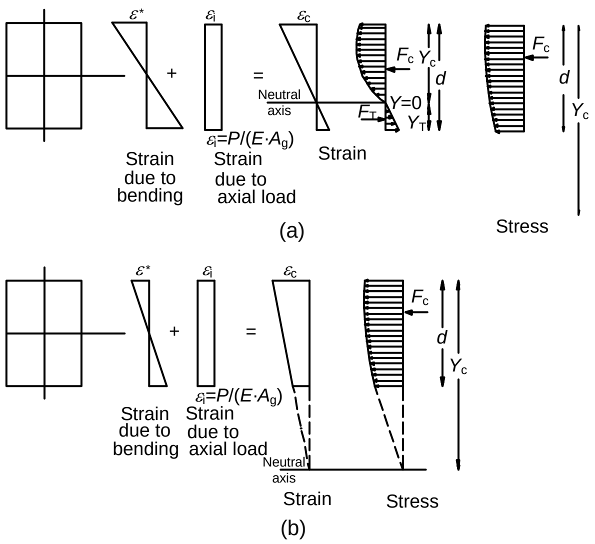

Fig. 12 Stage 1 in presence of axial load in compression state (a) and compression-tension state (b)

E: elastic modulus; A_g: cross section area

Now considering the equilibrium law ($F_c=P_1$), the neutral axis position can be determined by changing the depth of compression region in the specified compression strain. The moment capacity of the section is also calculated by

$$M_{\mathrm{Total}} = M_c, \quad (22)$$

$$M_c = \int_0^{Y_c} \sigma_c by\mathrm{d}y = \int_0^{Y_c} f_c'[2Y/Y_0-(Y/Y_0)^2]by\mathrm{d}y. \quad (23)$$

Applied axial load (P_1) should be considered in the equilibrium of the section forces. The procedure given in Fig. 6 shall be modified as shown in Fig. 13.

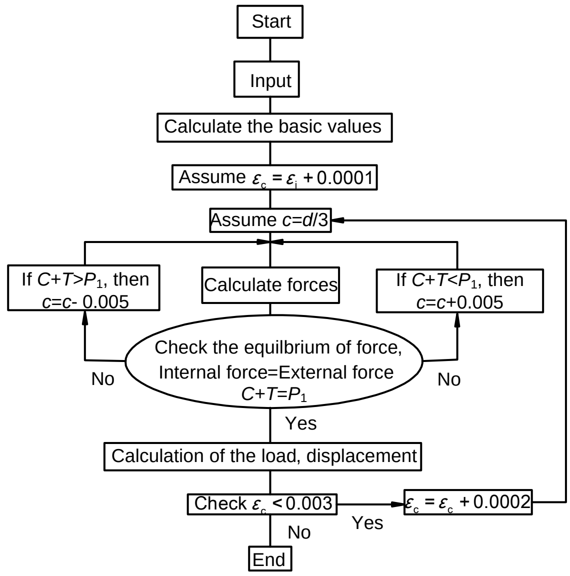

Fig. 13 Modified step by step procedure for generating the load-deflection curve in presence of axial load

C: compressive force; T: tension force; c: compressive depth; d: depth of section; P_1: applied axial load; ε_i: strain due to initial load

One set of parametric studies was conducted to evaluate this formulation (Fig. 14). The initial load results in growth in the amount of the bending load and reduction in the ultimate deflection capacity.

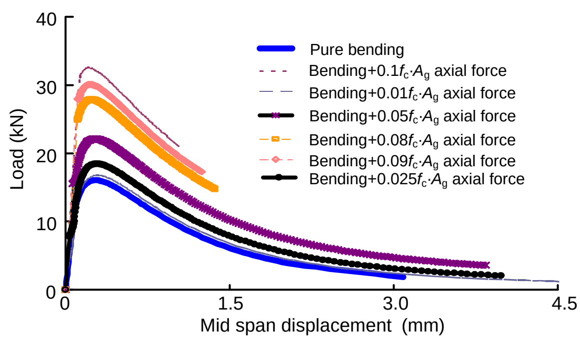

Fig. 14 Load-deflection for a fiber reinforced concrete material in presence of initial axial load

6 Conclusions

A precise solution has been presented to predict the behavior of FRC material under FPBT. A realistic stress-strain model is used for the concrete behavior in compression, and a linear response is considered for the uncracked tension region as a concrete constitutive model. An exponential relationship is proposed as a stress-crack opening in the crack region. The proposed model is simple and can be easily formulated. After that, parametric studies on the behavior of SFRC are done to assess the sensitivity of the model. Finally, the proposed model is validated through existing experimental results. The results show proper agreement with experimental data. This model can be completed further by using appropriate assumptions for the crack opening relationship.

References

Abdalla, H.M., Karihaloo, B.L., 2004. A method for constructing the bilinear tension softening diagram of concrete corresponding to its true fracture energy. *Magazine of Concrete Research*, **56**(10):597-604. [doi:10.1680/macr.2004.56.10.597]

Armelin, H.S., Banthia, N., 1997. Predicting the flexural post cracking performance of steel fiber reinforced concrete from the pullout of single fibers. *ACI Materials Journal*, **94**(1):18-31.

ASTM C1018-97, 1997. Standard Test Method for Flexural Toughness and First-Crack Strength of Fibre-Reinforced Concrete. American Society for Testing and Materials, USA. Available from http://www.astm.org/Standards/C1018.htm [Accessed on Apr. 9, 2011].

Balaguru, P., Najm, H., 2004. High-performance fiber-reinforced concrete mixture proportions with high fiber volume fractions. *ACI Materials Journal*, **101**(4):281-286.

Banthia, N., Trottier, J.F., 1995. Test methods for flexural toughness characterization of fiber reinforced concrete: some concerns and proposition. *ACI Materials Journal*, **92**(1):48-57.

JCI SF4, 1983. Standards for Test Methods of Fibre Reinforced Concrete, Method of Test for Flexural Strength and Flexural Toughness of Fibre Reinforced Concrete. Japanese Concrete Institute, p.45-51.

Li, V.C., 2002. Large volume, high-performance applications of fibers in civil engineering. *Journal of Applied Polymer Science*, **83**(3):660-686. [doi:10.1002/app.2263]

Mobasher, B., Shah, S.P., 1989. Test parameters for evaluating toughness of glass fiber reinforced concrete panels. *ACI Materials Journal*, **86**(5):448-458.

Mobasher, B., Li, C.Y., 1996. Mechanical properties of hybrid cement-based composites. *ACI Materials Journal*, **93**(3):284-292.

Oh, B.H., Kim, J.C., Choi, Y.C., 2007. Fracture behavior of concrete members reinforced with structural synthetic fibers. *Engineering Fracture Mechanics*, **74**(1-2):243-257. [doi:10.1016/j.engfracmech.2006.01.032]

Park, R., Paulay, T., 1975. Reinforced Concrete Structures. John Wiley and Sons, NY, USA. [doi:10.1002/9780470172834]

Prudencio, L., Austin, S., Jones, P., Armelin, H., Robins, P., 2006. Prediction of steel fibre reinforced concrete under flexure from an inferred fibre pull-out response. *Materials and Structures*, **39**(6):601-610. [doi:10.1617/s11527-006-9091-2]

RILEM TC 162-TDF, 2001. Uni-axial tension test for steel fibre reinforced concrete. *Materials and Structures*, **34**:3-6.

Stang, H., Li, V.C., 2004. Classification of Fiber Reinforced Cementitious Material for Structural Applications. 6th RILEM Symposium of FRC, Varenna, Italy, p.197-218.

van Mier, J.G.M., van Vliet, M.R.A., 2002. Uniaxial tensile test for the determination of fracture parameters of concrete: state of the art. *Engineering Fracture Mechanics*, **69**(2):235-247. [doi:10.1016/S0013-7944(01)00087-X]

Zhang, J., Stang, H., 1998. Applications of stress crack width relationship in predicting the flexural behavior of fiber-reinforced concrete. *Cement and Concrete research*, **28**(3):439-452. [doi:10.1016/S0008-8846(97)00275-5]